JOURNAL OF CATALYSIS **159,** 107–111 (1996)
ARTICLE NO. 0069

Effect of Surface Area on the Oxidation of Methane over Solid Oxide Solution Catalyst $La_{0.8}Sr_{0.2}MnO_3$

N. Gunasekaran, S. Saddawi, and J. J. Carberry

Laboratory of Catalysis, Department of Chemical Engineering, University of Notre Dame, Notre Dame, Indiana 46556

Received August 18, 1995; accepted October 24, 1995

Solid oxide solutions of the type $La_{0.8}Sr_{0.2}MnO_3$ with BET surface areas of 28, 20, 12, and 8 m^2/g were prepared by sintering at 700, 800, 900, and 1000°C, respectively. The catalysts were tested for methane total oxidation in a fixed bed reactor with feed containing 0.28% CH_4, 12% O_2, and the balance helium. The activity of methane at 550°C was found to decrease from 0.7 μmol/s·g to 0.2 μmol/s · g with the decrease in the surface area (28 and 8 m^2/g, respectively) of $La_{0.8}Sr_{0.2}MnO_3$. Temperature programmed desorption studies indicate that the amount of oxygen desorbed on these $La_{0.8}Sr_{0.2}MnO_3$ oxides decreased from 15 to 0.8 μmol/g with the decrease in the surface area. X-ray photoelectron spectroscopy studies revealed a decrease in the Mn surface concentration for the samples sintered at 700 to 1000°C. The oxidation of methane on $La_{0.8}Sr_{0.2}MnO_3$ was found to correlate with the surface area, i.e., facile, the surface concentration of Mn, and the oxygen properties of the oxides. © 1996 Academic Press, Inc.

INTRODUCTION

Perovskite oxides of the type $La_{1-x}A_xMO_3$ have been widely tested for many catalytic applications (1–3). Considerable interest has been focused on the $LaMnO_3$-based perovskites for their use as electrode materials in high-temperature solid oxide fuel cells (4). It is generally known that increasing the surface area of oxide materials enhances their activity for many catalytic reactions. Therefore, several methods of obtaining oxides with high surface area and high catalytic activity, such as carbonate (5), citrate (6), and oxalate (7) precipitation or polymerization (8, 9) and freeze drying (10, 11), have been explored. Arai *et al.* (12) have studied the catalytic oxidation of methane over various perovskite type oxides and compared their activities with that of Pt/Al_2O_3. Among the oxide catalysts, they found the highest CH_4 oxidation activity with $La_{0.8}Sr_{0.2}MnO_3$ perovskite, a result comparable to that for the Pt catalyst. However, a significant decrease in the activity of Mn perovskite was noticed when the sintering temperature was increased from 850 to 1200°C. The influence of surface area on the catalytic activity has also been investigated for other reactions such as CO oxidation and propane oxidation (10, 13, 14).

We have previously investigated a series of solid oxide solutions (SOS) of the type $La_{0.8}Sr_{0.2}MO_3$ oxides (M = Cr, Mn, Fe, Co, or Y) for various catalytic reactions such as CO oxidation and propylene hydrogenation (15–17). In our continued interest in these SOS catalysts, we have developed a method of obtaining these oxides with high surface areas by optimizing the preparation conditions. A series of compounds of the formula $La_{1-x}Ba_xMnO_3$ with surface areas in the range of 30 m^2/g were prepared, which exhibit promising activity for methane oxidation (18). The concentrations of the reactant gases were chosen to complement our NO_x reduction studies using hydrocarbon in the presence of oxygen. Therefore the objectives of the present study are (i) to prepare $La_{0.8}Sr_{0.2}MnO_3$ of various surface areas by an optimized Pechini method, (ii) to establish the oxygen properties of the catalysts by temperature programmed desorption (TPD) studies, and (iii) to compare the activity of $La_{0.8}Sr_{0.2}MnO_3$ with our previous results for Ba-substituted $LaMnO_3$.

EXPERIMENTAL

$La_{0.8}Sr_{0.2}MnO_3$ was prepared by a method similar to that described previously; the details are available elsewhere (18). The resultant powder, obtained after calcination at 450°C, was divided into several portions and subjected to specific sintering temperatures for 4 h. A Diano X-ray diffractometer was used to identify the single-phase formation of the oxides using Cu$K\alpha$ radiation at a scan rate of 1°/min. For all sintering temperatures, the XRD analysis showed peaks corresponding to a perovskite structure. The surface areas of the samples were measured by the single-point BET method using a Quantachrome Monosorb (Model MS-16) analyzer. XPS studies were made with a Kratos XSAM 800 AUGER/ESCA system using Mg$K\alpha$ radiation as described in the previous paper (19).

The total oxidation of methane was carried out in a fixed bed flow reactor (18). A mixture of methane (0.28%), oxygen (12%), and helium (balance) was fed to the reactor at a flow rate of 70 cm^3/min. Product analysis was performed using gas chromatography with a Carbo-

0021-9517/96 $18.00
Copyright © 1996 by Academic Press, Inc.
All rights of reproduction in any form reserved.

sphere column (Alltech Associates, U.S.A). An excellent carbon balance for the product indicated that the major reaction products were only CO_2 and H_2O. Temperature programmed desorption of oxygen was recorded with a flow system using helium as a carrier gas. Prior to each experiment, the sample was heated in an oxygen stream from ambient temperature to 800°C. After being held at 800°C for 1 h, it was cooled to room temperature and then the gas flow was switched to helium. The sample was then heated at a programmed rate of 1°C/s and the oxygen desorbed was monitored using a thermal conductivity detector.

RESULTS AND DISCUSSION

X-ray diffraction analysis indicated that all four SOS ($La_{0.8}Sr_{0.2}MnO_3$) possess perovskite peaks. The *d*-spacings were compared with those of unsubstituted $LaMnO_3$. The XRD patterns of $La_{0.8}Sr_{0.2}MnO_3$ were very similar to that of Ba-substituted SOS (18). The XPS spectra for the La 3*d*, Sr 3*d*, Mn 2*p*, and O 1*s* levels were recorded for $La_{0.8}Sr_{0.2}MnO_3$ samples sintered at 700, 800, 900, and 1000°C. A typical XPS spectrum for the sample sintered at 700°C is shown in Fig. 1. The peak characteristics of the La 3*d*, Sr 3*d*, Mn 2*p*, and O 1*s* levels were identical in all samples and the binding energy values given in Table 1 were in good agreement with those reported in the literature (19–21). However, a distinct variation in the intensity of La 3*d*, Sr 3*d*, and Mn 2*p* was observed with the samples sintered between 700 and 1000°C. The areas under the La $3d_{5/2}$, Sr $3d_{5/2}$, and Mn $2p_{3/2}$ peak positions were analyzed to obtain the surface concentration ratio of each element using a quantification method incorporated in the instrument software. Further details on the La and Mn peak characteristics are available elsewhere (19). The O 1*s* spectra showed similarity in all of the four sintered samples with a doublet peak of binding energy at 529 and 531 eV. From the literature data, the peak at lower binding energy (529 eV) can be assigned to the lattice oxygen (metal–oxygen bond) and the peak at 531 eV is due to the absorbed/adsorbed oxygen (19, 20). The peak position, the factor, and the atomic concentration of each element are given in Table 1. As seen from Table 1 the sample sintered at low temperature (700°C) showed a maximum Mn concentration and a gradual decrease was observed with the samples sintered at 800 to 1000°C. One reason for the change in the surface composition with sintering has been suggested to be the free energy of formation of component oxides. Tabata *et al.* (20) have observed a similar trend in the surface composition with the $La_{1-x}Sr_xCoO_3$ system. They reported the ΔG values of La_2O_3, Co_3O_4, and SrO as −1254.2, −769.3, and −561.9 kJ/mol, respectively. Both Co and Sr, whose free energy values are smaller than that of La, seemed to reveal a decrease in surface concentration during calcination. Using the thermochemical data of Kubaschewski *et al.* (22) the free energy (ΔG) values obtained for La_2O_3 and MnO are −1748.6 and −362.7 kJ/mol, respectively. Based on the ΔG values one would expect the Mn concentration to decrease with the increase in sintering temperature, as indeed has been realized in our $La_{0.8}Sr_{0.2}MnO_3$ samples.

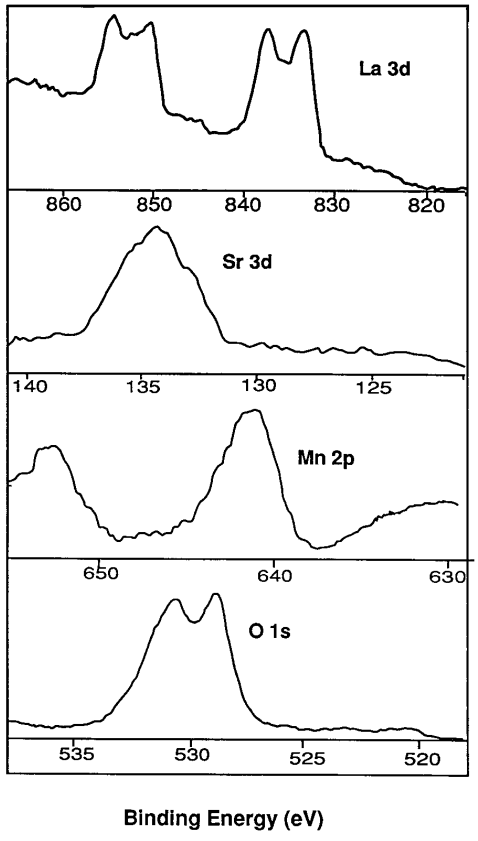

FIG. 1. Typical X-ray photoelectron spectra of $La_{0.8}Sr_{0.2}MnO_3$ sintered at 700°C.

TABLE 1

XPS Binding Energy Values and Surface Composition of $La_{0.8}Sr_{0.2}MnO_3$

Region	700[a]	800[a]	900[a]	1000[a]
La $3d_{5/2}$	833.6	833.5	833.1	833.8
Sr $3d_{5/2}$	137.8	134.3	133.7	133.8
Mn $2p_{3/2}$	641.4	641.8	641.3	641.2
O 1*s*	528.2; 531.4	528.7; 531.7	528.9; 531.2	528.5; 531.6
La[b]	46.5	46.0	44.3	53.9
Sr[b]	16.7	23.6	25.9	24.8
Mn[b]	36.8	30.4	29.8	21.3
C_{Mn}[c]	0.58	0.44	0.42	0.27

[a] $La_{0.8}Sr_{0.2}MnO_3$ samples sintered at 700, 800, 900, and 1000°C with BET surface area of 28, 20, 12, and 8 m^2/g, respectively.
[b] Surface concentration of each element in percentage.
[c] Refers of Mn/(La + Sr)

TABLE 2

Physicochemical and Catalytic Properties of $La_{0.8}Sr_{0.2}MnO_3$ for Methane Oxidation Reaction

Sintering temperature (°C)	BET surface area (m^2/g)	Conversion[a] (%)	Activity (μmol/s · g)	Specific activity (μmol/s · m^2)	E_a[b] (kcal/mol)	Amount of oxygen desorbed (μmol/g)
700	28	50	0.68	0.02	9.16	15.66
800	20	30	0.41	0.02	37.70	11.54
900	12.5	25	0.34	0.03	14.04	3.77
1000	8	16	0.22	0.03	18.53	0.87

Note. Feed mixture: 0.28% methane, 12% oxygen, and balance helium. Feed flow rate: 70 cm^3/min.

[a] Data correspond to temperature of 550°C.

[b] Values are computed from rate obtained below 10% conversion level.

The BET surface areas of the SOS ($La_{0.8}Sr_{0.2}MnO_3$) are listed in Table 2. The surface area of the catalysts before and after the reaction showed a difference of ±3 m^2/g, which is within the experimental error involved in the measurement technique. It can be seen that the sample sintered at relatively low temperature (700°C) showed the highest surface area, 28 m^2/g, a similar result has been reported for the $La_{1-x}Ba_xMnO_3$ system (18). Although it is expected that these types of Mn SOS can be prepared at sintering temperatures as low as 600°C (6), such an attempt has not been made in the present study since the reaction temperature for methane oxidation proceeds above 600°C on many oxide catalysts. It is to be noted that the surface area of $La_{0.8}Sr_{0.2}MnO_3$ remained almost constant (28 to 25 m^2/g) with the time of sintering (4 to 48 h, respectively) at 700°C, whereas a linear decrease (28 to 8 m^2/g) was noted with an increase in the sintering temperature (700 to 1000°C). This indicates that sintering temperature, and not sintering time, is critical in the preparation of these oxides with high surface area. Kirchnerova *et al.* (11) have also arrived at the same conclusion for the various mixed oxides prepared by freeze-drying techniques.

The methane oxidation activity of $La_{0.8}Sr_{0.2}MnO_3$ with different surface areas is depicted in the form of light-off temperature (LOT) curves in Fig. 2, where LOT is the temperature of the reaction initiation. As Fig. 2 indicates, there is a gradual decrease in the LOT of methane oxidation (increase in activity) with an increase in the surface area of the oxides. Methane oxidation occurs at around 300°C on these types of SOS and complete oxidation is evident at about 600°C. However, the SOS with low surface area (sample sintered at 1000°C) exhibits only 60% methane conversion at 600°C. The thermal uncatalyzed data obtained in this study under the same experimental conditions have been included in Fig. 2. The thermal data are in excellent agreement with those reported by Arai *et al.* for methane oxidation (12). The activity data and the corresponding values of activation energy for the four $La_{0.8}Sr_{0.2}MnO_3$ oxides are provided in Table 2. The average rate of methane oxidation is approximated using the equation

$$\text{Rate} = C_f \cdot \chi/\theta,$$

where C_f is the feed concentration, χ is the fraction of methane converted at a given temperature, and θ is the residence time (W/F). The rates at differential (i.e., CSTR) conditions for conversions below 10% were used to obtain activation energy values. A comparison of the Arrhenius plot for these four SOS with differing surface areas is shown in Fig. 3. The E_a values for the samples are in the range of 10–20 kcal/mol (Table 2) and thus are in fairly good agreement with other reported values (12).

The TPD of oxygen for $La_{0.8}Sr_{0.2}MnO_3$ samples is presented in Fig. 4. As was observed with our $La_{1-x}Ba_xMnO_3$ system (18), two prominent oxygen peaks are found in this

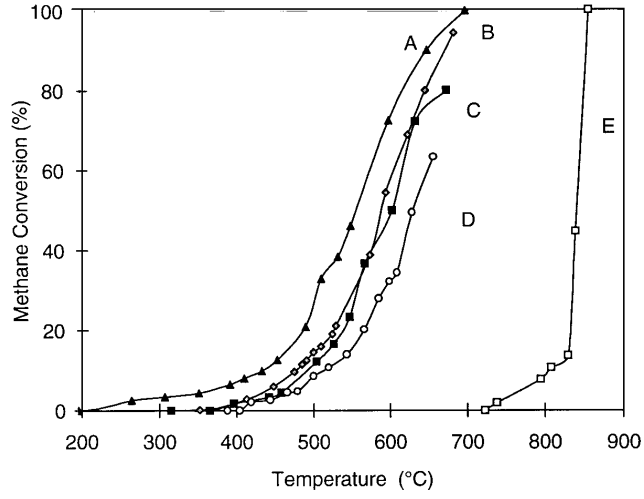

FIG. 2. Light-off temperature curves for the oxidation of methane over $La_{0.8}Sr_{0.2}MnO_3$ with different surface areas. Curves A, B, C, and D correspond to BET surface areas of 28, 20, 12, and 8 m^2/g, respectively. Curve E represents thermal reaction without catalyst. Experimental conditions: Total flow rate, 70 cm^3/min. Feed, 0.28% methane, 12% oxygen, and balance helium. Catalyst weight, 0.1 g.

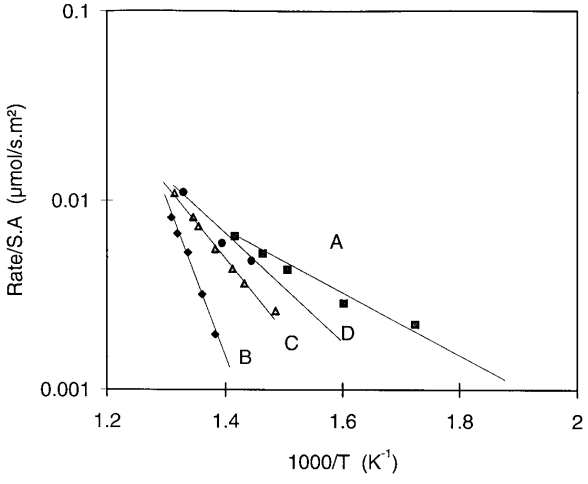

FIG. 3. Arrhenius plot for the methane oxidation over $La_{0.8}Sr_{0.2}MnO_3$ oxides. A, B, C, and D correspond to samples with surface areas of 28, 20, 12, and 8 m^2/g, respectively.

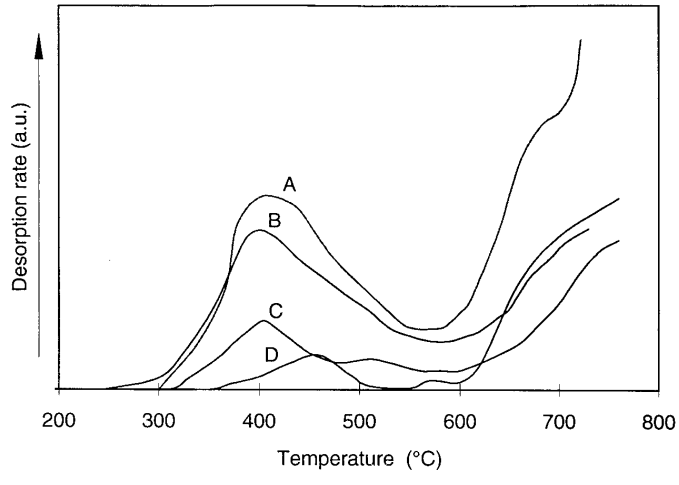

FIG. 4. TPD profiles of oxygen for $La_{0.8}Sr_{0.2}MnO_3$ sintered at different temperatures. Curves A, B, C, and D correspond to sintering temperatures of 700, 800, 900, and 1000°C, respectively.

study with temperature maxima at around 410°C and above 700°C. We focused our attention on the analysis of peak 1 since the methane oxidation reaction was performed in the temperature range 200 to 650°C on these oxides. The calculated values of the amount of oxygen desorbed (under peak 1) on the four $La_{0.8}Sr_{0.2}MnO_3$ samples are presented in Table 2. Although a similar trend in the oxygen TPD spectrum has been reported for $La_{0.8}Sr_{0.2}MnO_3$ by Petrolekas and Metcalfe (23) and Nitadori *et al.* (14) the amount of desorbed oxygen was found to vary significantly in this study from the amounts reported in Refs. (14) and (23). This could be due to the different method of preparation employed to obtain the $La_{0.8}Sr_{0.2}MnO_3$ oxide.

In Fig. 4 we see a continuous decrease in oxygen desorption (15 to 0.8 μmol/g) with increased sintering temperature (i.e., decreased surface area). Further, the peak maximum (peak 1) was found to shift from 390 to 460°C with the decreases in the surface area of the oxide. This shift in the desorption temperature indicates that the oxygen species exist as different types (O^-, O^{2-}, etc.) and strengths on these SOS ($La_{0.8}Sr_{0.2}MnO_3$). Furthermore, we observe a linear relationship between the amount of oxygen desorbed and the surface concentration of Mn (ratio of Mn/La + Sr) as revealed by XPS study. Therefore the activity of methane oxidation and the oxygen properties are related to the surface concentration of the Mn in the $La_{0.8}Sr_{0.2}MnO_3$ samples.

The influence of Sr^{2+} and Ba^{2+} substitution for La in $LaMnO_3$ in the catalytic activity of methane oxidation is shown in Fig. 5 (see curves B and A, respectively). These Sr and Ba solid solution samples were prepared and tested under identical experimental conditions. The data for methane activity, oxygen properties, and surface areas are given in Table 3. From Fig. 5 one notes that methane conversions are much higher for the $La_{0.8}Ba_{0.2}MnO_3$ than for the Sr SOS (75 and 50%, respectively, at 550°C). From the XPS analysis, the surface concentrations of Mn (Mn/(La + alkaline earth metal) in $La_{0.8}Ba_{0.2}MnO_3$ and $La_{0.8}Sr_{0.2}MnO_3$ were found

TABLE 3

Comparison of Activity on Some Manganese Catalysts for Methane Oxidation at 550°C

Catalyst	Method of preparation	Sintering temperature (°C)	BET S.A. (m^2/g)	Conversion (%)	Activity (μmol/s · g)	Sp. activity (μmol/s · m^2)	Amount of oxygen desorbed (μmol/g)	Ref.
$La_{0.8}Sr_{0.2}MnO_3$	Pechini	700	28.00	50.00	0.68	0.02	15.7	This work
$La_{0.8}Ba_{0.2}MnO_3$	Pechini	700	31.00	75.00	0.95	0.03	92	18[a]
$La_{0.8}Sr_{0.2}MnO_3$	Pechini	1000	8	16	0.22	0.03	0.87	This work
$La_{0.8}Sr_{0.2}MnO_3$	Solid state	1000	1.40	15.00	0.80	0.57	—	15[a]
$LaMnO_3$	Pechini	700	33.00	60.00	0.76	0.02	156	18[a]
$LaMnO_3$	Acetate	850	4.00	40.00	2.80	0.7	—	12

[a] Our previous work.

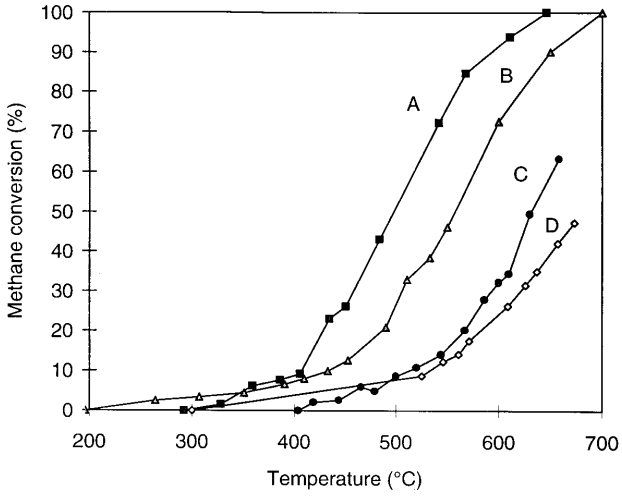

FIG. 5. Effect of *A*-site substitution on $La_{0.8}A_{0.2}MnO_3$ (A = Sr or Ba) and method of preparation of $La_{0.8}Sr_{0.2}MnO_3$ for the oxidation of methane. Curves A and B correspond to $La_{0.8}Ba_{0.2}MnO_3$ (A) and $La_{0.8}Sr_{0.2}MnO_3$ (B) (700°C sintering). Curves C and D refer to $La_{0.8}Sr_{0.2}MnO_3$ prepared by the Pechini (C) and solid state methods (D) (1000°C sintering).

to be 0.76 (18) and 0.58, respectively. This may well explain the superior behavior of the Ba compound in methane oxidation relative to that of $La_{0.8}Sr_{0.2}MnO_3$. Yamashita *et al.* (24) have demonstrated that peroxide-type oxygen species (O_2^{2-}) are responsible for the oxidative coupling of methane over Ba–La–O systems. Kharas and Lunsford (25) have also suggested the role of peroxide species on $BaPbO_3$ in the methane coupling reaction. Such phenomena have not been observed with the Sr-containing compounds. Therefore the increase in the amount of oxygen desorbed (92 μmol/g) observed with $La_{0.8}Ba_{0.2}MnO_3$ could well be due to the combined effect of Ba peroxide formation and the higher surface concentration of Mn in Ba SOS relative to $La_{0.8}Sr_{0.2}MnO_3$.

A shift in the light-off temperature (variation in catalytic activity) for a given reaction has been generally found to depend on the method of preparation and the sintering temperature of the oxides (11–13). In Fig. 5 the effect of the method of preparation on $La_{0.8}Sr_{0.2}MnO_3$ for the methane oxidation reaction is illustrated. Accordingly, LOT curves C and D represent the sample prepared by the Pechini (this study) and solid state methods (from Ref. 15), respectively. A significant activity difference due to the method of preparation is observed only above the 30% conversion level. The available activity data for the unsubstituted $LaMnO_3$ compositions are also included in Table 3 for reference.

CONCLUSION

$La_{0.8}Sr_{0.2}MnO_3$ with a high surface area (28 m^2/g) was prepared using the Pechini method at a relatively low sintering temperature (700°C). The surface area was found to decrease from 28 to 8 m^2/g when the sintering temperature was raised from 700 to 1000°C. The catalytic activity for methane oxidation on these SOS was found to decrease with the decrease in the surface area, which correlates well with the oxygen TPD results and the surface compositions of Mn as ascertained by XPS studies.

REFERENCES

1. Seiyama, T., *Catal. Rev. Sci. Eng.* **34**, 281 (1992).
2. Tejuca, L. G., Fierro, J. L. G., and Tascon, J. M. D., *Adv. Catal.* **36**, 237 (1989).
3. Carberry, J. J., Rajadurai, S., Li, B., and Alcock, C. B., *Catal. Lett.* **4**, 43 (1990).
4. Grosz, F., Zegers, P., Singhal, S. C., and Yamato, O. (Eds.), "Proceedings of 2nd International Symposium on Solid Oxide Fuel Cells, Athens, July 1991."
5. Raj, S. Louis, and Srinivasan, V., *J. Catal.* **65**, 121 (1980).
6. Zhang, H., Teraoka, Y., and Yamazoe, N., *Chem. Lett.* 665 (1987).
7. Nakamori, T., Abe, H., Takahashi, Y., Kanamori, T., and Shibata, S., *Jpn. J. Appl. Phys.* **27**, L649 (1988).
8. Pechini, M. P., U.S. Patent 3,330,697 (1967).
9. Lessing, P. A., *Ceram. Bull.* **68**, 1002 (1989).
10. Johnson, D. W., Gallagher, P. K., Schrey, F., and Rhodes, W. W., *Ceram. Bull.* **55**, 520 (1976).
11. Kirchnerova, J., Klvana, D., Vaillancourt, J., and Chaouki, J., *Catal. Lett.* **21**, 77 (1993).
12. Arai, H., Yamada, T., Eguchi, K., and Seiyama, T., *Appl. Catal.* **26**, 265 (1986).
13. Barnard, K. R., Foger, K., Turney, T. W., and Williams, R. D., *J. Catal.* **125**, 265 (1990).
14. Nitadori, T., Kurihara, S., and Misono, M., *J. Catal.* **98**, 221 (1986).
15. Doshi, R., Alcock, C. B., Gunasekaran, N., and Carberry, J. J., *J. Catal.* **140**, 557 (1993).
16. Alcock, C. B., Doshi, R., Carberry, J. J., and Gunasekaran, N., *J. Catal.* **143**, 553 (1993).
17. Gunasekaran, N., Carberry, J. J., Doshi, R., and Alcock, C. B., *J. Catal.* **146**, 583 (1994).
18. Gunasekaran, N., Rajadurai, S., Carberry, J. J., Bakshi, N., and Alcock, C. B., *Solid State Ionics,* in press.
19. Gunasekaran, N., Rajadurai, S., Carberry, J. J., Bakshi, N., and Alcock, C. B., *Solid State Ionics* **73**, 289 (1994).
20. Tabata, K., Matsumato, I., and Kohiki, S., *J. Mater. Sci.* **22**, 1882 (1989).
21. Oku, M., and Hirokawa, K., *J. Electr. Spectrosc. Relat. Phenom.* **8**, 475 (1976).
22. Kubaschewski, O., Spencer, P. J., and Alcock, C. B., "Materials Thermochemistry," 6th edition. Pergamon, Elmsford, NY, 1993.
23. Petrolekas, P. D., and Metcalfe, I. S., *J. Catal.* **152**, 147 (1995).
24. Yamashita, H., Machida, Y., and Tomita, A., *Appl. Catal.* **79**, 203 (1991).
25. Kharas, K. C. C., and Lunsford, J. H., *J. Am. Chem. Soc.* **111**, 2336 (1989).